Advancements in cardiovascular imaging: serial coronary CT and myocardial CT perfusion quantification techniques

Driest, F.Y. van

6 Comparison of left ventricular mass and wall thickness between cardiac computed tomography angiography and cardiac magnetic resonance imaging using machine learning algorithms

Finn Y van Driest
Rob J van der Geest
Sharif K Omara
Alexander Broersen
Jouke Dijkstra
J Wouter Jukema
Arthur J H A Scholte

Abstract

Introduction: Cardiac magnetic resonance imaging (MRI) is the gold standard in the assessment of left ventricle (LV) mass and wall thickness. In recent years, cardiac computed tomography angiography (CCTA) has gained widespread usage as an imaging modality. Despite this, limited previous investigations have specifically addressed the potential of CCTA as an alternative modality for quantitative LV assessment.

The aim of this study was to compare CCTA derived LV mass and wall thickness with cardiac MRI utilizing machine learning algorithms.

Methods: Fifty-seven participants who underwent both CCTA and cardiac MRI were identified. LV mass and wall thickness was calculated using LV contours which were automatically placed using in-house developed machine learning models. Pearson's correlation coefficients were calculated along with Bland-Altman plots to assess the agreement between the LV mass and wall thickness per region on CCTA and cardiac MRI. Inter-observer correlations were tested using Pearson's correlation coefficient.

Results: Average LV mass and wall thickness for CCTA and cardiac MRI were 127 g ,128 g, 7 and 8mm respectively. Bland-Altman plots demonstrated mean differences and corresponding 95% limits of agreement of -1.26 (25.06;-27.58) and -0.57 (1.78;-2.92), for LV mass and average LV wall thickness, respectively. Mean differences and corresponding 95% limits of agreement for wall thickness per region were -0.75 (1.34;-2.83), -0.58 (2.14;-3.30) and -0.29 (3.21;-3.79) for the basal, mid, and apical regions, respectively. Inter-observer correlations were excellent.

Conclusion: Quantitative assessment of LV mass and wall thickness on CCTA using machine learning algorithms seems feasible and shows good agreement with cardiac MRI.

Abbreviations

AI: Artificial Intelligence
CCTA: Cardiac computed tomography angiography
DICOM: Digital Imaging and Communications in Medicine
ECG: Electrocardiogram
FOV: Field of view
HU: Hounsfield units
LV: Left ventricle
MRI: Magnetic resonance imaging
RV: Right ventricle
TE: Echo time
TR: Repetition time

1. Introduction

Increased left ventricle (LV) mass and wall thickness causing LV hypertrophy are both independent risk factors for cardiovascular mortality and morbidity irrespective of the aetiology (1). Cardiac magnetic resonance imaging (MRI) is still considered to be the gold standard for LV mass and wall thickness measurements (2). However, over the years cardiac computed tomography angiography (CCTA) has become a widely used imaging modality for the assessment of coronary arteries and its diagnostic accuracy has greatly increased in the last decade (3). Still, only a few prior studies have been performed about the use of CCTA for LV mass and wall thickness measurements and only a minor number have compared the measurements to MRI (4-10). Nasser Alnasser et al. have written an extensive review about the use of artificial intelligence (AI) in (cardiac) structure segmentation (11) however, to the best of our knowledge no prior study has incorporated the use of machine-learning-based LV segmentation into the comparison of CCTA and MRI derived LV mass and wall thickness measurements. Use of CCTA for LV mass and wall thickness measurements may be especially useful for patients with contraindications for cardiac MRI such as pacemakers, claustrophobia, or clinical conditions that prohibit long MRI examinations (9). Furthermore, CCTA has been proven to be more readily available, cheaper and faster as compared to MRI (12, 13)

Quantification of LV mass and wall thickness requires the definition of LV endo- and epicardial contours in multiple slices covering the complete LV. Manual segmentation of the LV myocardium is time consuming both for CCTA and cardiac MRI (14, 15). Recently, machine learning algorithms have been developed for both CCTA and cardiac MRI and allow for automatic LV segmentation substantially decreasing the time needed for LV quantification (14, 16, 17). The aim of this study was to compare LV mass and LV wall thickness derived from CCTA and cardiac MRI whilst using machine learning based LV segmentation.

2. Materials and methods

2.1 Patients

For this study 130 participants who underwent both CCTA and cardiac MRI between October 2009 and November 2021 were identified. Participants with a maximum period of more than 6 months between CCTA and cardiac MRI (n = 59), no short-axis cine magnetic resonance (MR) image stack (n = 9), severe motion artifacts on MRI (n = 1), CCTA without contrast (n = 3) and corrupt CCTA digital imaging and communications in medicine (DICOM) files (n = 1) were excluded. A total of 57 participants were selected for the current analysis. Among them, thirteen exhibited LV hypertrophy. Patient characteristics and indications for CCTA and cardiac MRI are described in Table 1. Figure 1 depicts a detailed flowchart of the patient selection. All data were analysed retrospectively. The local ethics

committee of the Leiden University Medical Centre approved this retrospective analysis of clinical data and waived the need for informed consent.

Table 1. Patient characteristics. CCTA: Cardiac computed tomography angiography. VT: Ventricular tachycardia. LV: Left ventricle

Patient characteristics	N = 57
Male / Female	43 (75%) / 14 (25%)
Age (years)	60 ± 12.2
Hypertension	24 (42%)
Hyperlipidaemia	12 (21%)
Diabetes mellitus	3 (5%)
Smoking	2 (4%)
LV hypertrophy*	13 (23%)
CCTA indication	
Chest pain	33 (58%)
Coronary anatomy for workup to VT ablation	22 (39%)
Aortic aneurysm	1 (2%)
Bicuspid aortic valve	1 (2%)
Cardiac MRI indication	
Cardiomyopathy	43 (75%)
Myocarditis	4 (7%)
Cardiac ischemia	3 (5%)
Sarcoidosis with cardiac involvement	3 (5%)
Aortic aneurysm	2 (4%)
Amyloidosis	1 (2%)
Bicuspid aortic valve	1 (2%)

*An end-diastolic LV wall thickness of more than 15mm as measured with 2D echocardiography or cardiac MRI anywhere in the left ventricle (32).

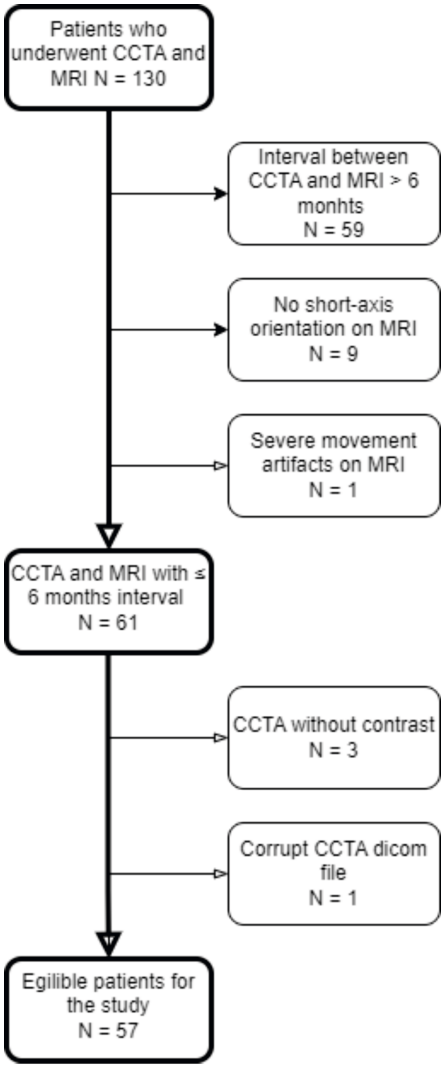

Figure 1. Flowchart demonstrating patient selection. Scans with an inter-scan interval of more than 6 months between MRI and CCTA were excluded. CCTA, cardiac computed tomography angiography. DICOM, digital imaging and communications in medicine. MRI, magnetic resonance imaging.

2.2 CCTA Data acquisition

CCTA was performed using a 320-row volumetric scanner (Aquilion ONE , Canon Medical Systems, Aquilion ONE PRISM Edition, Canon Medical Systems and Aquilion ONE Genesis Edition, Canon Medical Systems, Otawara, Japan). A peak tube voltage of 100-135 kV with a tube current of 140-580mA was used. Detector collimation, gantry rotation time and temporal resolution were 320 x 0.5mm, 275ms and 137ms, for the Aquilon ONE Genesis Edition and 320 x 0.5mm, 350ms and 175ms, for the Aquilon ONE (PRISM Edition)

respectively. The antecubital vein was used for administration of 50–90 mL of contrast agent (Iomeron 400, Bracco, Milan, Italy) followed by a 1:1 mixture of 20 mL contrast and saline and finally 25 mL of saline. Peak tube voltage, tube current and amount of contrast agent varied based on patient size (18). After contrast administration CCTA was performed the next heartbeat when a threshold of 300 Hounsfield units was reached in the descending aorta. Subsequently, 70-80% of the RR interval was scanned using prospective electrocardiogram (ECG) triggering.

2.3 MRI Data acquisition

Cardiac MRI was performed using a 1.5-T Gyroscan ACS-NT/Intera MR system (Philips Medical Systems, Best, The Netherlands) or a 3.0-T Ingenia MR system (Philips Medical Systems, Best, The Netherlands) using retrospective ECG gating. Imaging parameters were as follows for the 1.5-T Gyroscan ACS-NT/Intera MR system: field of view (FOV) 400 × 320 mm^2; matrix, 256 × 206 pixels; slice thickness, 10 mm with no slice gap; flip angle (α), 35°; echo time (TE), 1.67 ms; and repetition time (TR), 3.3 ms. For the 3.0-T Ingenia MR system typical parameters were: FOV 400 × 350 mm; matrix, 232 × 192 pixels; slice thickness, 8 mm with no slice gap; α, 45°; TE, 1.5 ms and TR, 3.0 ms. The heart was imaged in 1 or 2 breath-holds with short-axis slices at various levels dependent on the heart size.

2.4 Image processing

Images were transferred to a workstation for quantitative analysis. In-house developed MASS software (Leiden University Medical Centre) was used for short-axis reformatting in the CCTA scans and for LV contour placement in the CCTA and MRI scans. The software has been validated and supported for clinical purposes. A study by Kawel provides robust evidence of its efficacy and reliability (19).

CCTA and MRI data were analysed independently and no visual reference to the other could be made at any time. Also, the observer was blinded to the results of LV mass and LV wall thickness of each scan. Quantitative analysis of both modalities as well as short-axis reformatting in the CCTA was done automatically by using machine learning models. Contours were manually corrected if needed. The AI model used for MRI and CCTA based LV segmentation used a deep learning-based approach. Specifically, a convolutional neural network architecture, known as the U-Net, was employed for this purpose. The AI model was trained on a large dataset of cardiac MRI and CCTA scans, where both the raw images and manually annotated LV contours are provided as input. During the training process, the model learns to map the input images to the corresponding LV contours, optimizing its parameters to minimize the difference between the predicted and ground truth segmentations. Finally, the performance of the AI model was evaluated on an independent testing dataset, which consists of additional cardiac MRI and CCTA scans. The model's predictions on the testing set were compared against manual ground truth annotations to assess its performance in real-world scenarios. Training and use of the

machine learning models is discussed in more detail for both CCTA and cardiac MRI in two separate papers (16, 17).

First, CCTA images were automatically reformatted into a short-axis orientation covering the complete LV with a slice thickness of 4 mm. Cardiac MRI images with a slice thickness of 8 or 10 mm were already available in short axis hence, no further reformatting was needed. Once short-axis slice stacks were created a reference point was placed in a mid-slice at the site of the inferior attachment of the right ventricle (RV) to LV, both for CCTA and cardiac MRI. The segment numbering within a specific level depends on the location of the reference point. Hence, this allows for anatomical alignment of CCTA and cardiac MRI. Finally, LV epicardial and endocardial contours were automatically detected first in the CCTA and hereafter in the cardiac MRI for each patient. The 75% phase was chosen for LV segmentation on both the CCTA and cardiac MRI as this phase is most ideal for LV mass and wall thickness calculation (20). Figure 2 depicts the results of LV segmentation for both CCTA and cardiac MRI.

We have opted not to include LV volume as the basis for its calculation (as is with LV mass) is based on endo- and epicardial LV contours using MASS software. As the main goal of this study was to evaluate the matter of agreement between CCTA and MRI derived LV contours we chose LV mass as a derivative of these contours. Therefore, including a comparison of LV volume between imaging modalities will not provide additional meaningful insights beyond what is already captured in the LV mass calculation process.

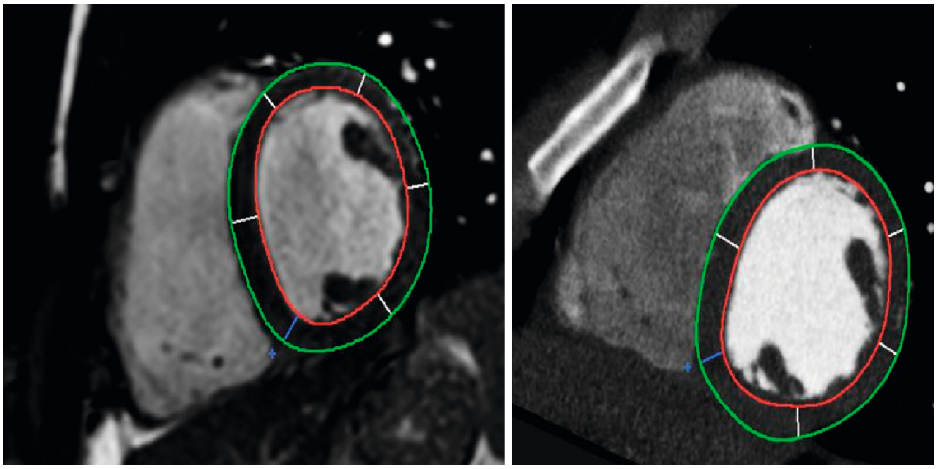

Figure 2. Example of LV segmentation of a middle region slice of the same patient for both cardiac MRI (left panel) and CCTA (right panel). The red lines represent the endocardial contours. The green lines represent the epicardial contours. The reference point is marked by the small blue cross. Middle region wall thickness for this patient was 8 mm on MRI and 6 mm on CCTA.

2.5 LV mass and wall thickness calculation

Using the LV contours, LV mass and wall thickness were calculated automatically using the aforementioned software. Average LV wall thickness as well as segmental wall thickness, using the standard 16-segment model were derived (21). Furthermore, segments were combined to provide wall thickness per LV region consisting of the basal, mid and apical regions (21) which is depicted in Figure 3. LV wall thickness for the entire LV and per region were calculated using the following formulas.

$$LV\,wall\,thickness = \frac{\text{segment } 1 + \text{segment } 2 + \ldots + \text{segment}16}{16}$$

$$LV\,wall\,thickness\,basal = \frac{\text{segment } 1 + \text{segment } 2 + \text{segment } 3 + \text{segment } 4 + \text{segment } 5 + \text{segment } 6}{6}$$

$$LV\,wall\,thickness\,mid = \frac{\text{segment } 7 + \text{segment } 8 + \text{segment } 9 + \text{segment } 10 + \text{segment } 11 + \text{segment } 12}{6}$$

$$LV\,wall\,thickness\,apical = \frac{\text{segment } 13 + \text{segment } 14 + \text{segment } 15 + \text{segment } 16}{4}$$

To assess inter-observer reproducibility a second independent observer performed quantitative analysis in a randomly selected cohort of twenty subjects. Since manual adjustments to the automatically detected contours was occasionally required, the results between observers may vary. Correlations of LV mass and LV wall thickness for both CCTA and cardiac MRI between both observers were subsequently tested using Pearson's correlation coefficient.

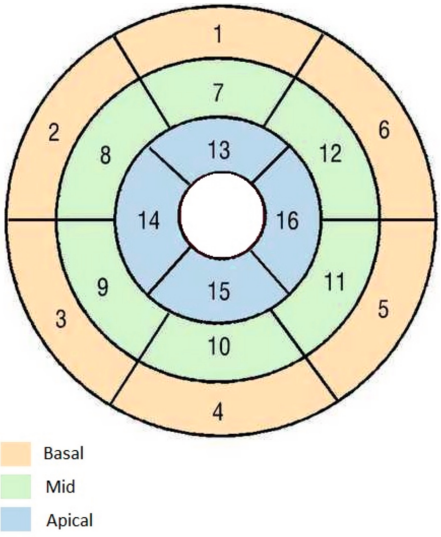

Figure 3. Standard 16-segment model depicting how different segments make up 3 different major regions; basal, mid and apical.

2.6 Statistical analysis

The agreement between LV mass and wall thickness derived from CCTA and cardiac MRI was assessed using Bland-Altman plots and Pearson's correlation coefficient. Inter-observer correlations were tested using Pearson's correlation coefficient. SPSS software version 25, SPSS IBM Corp, Armonk, New York) was used for all statistical analysis.

3. Theory

Performing a comparison of CCTA and LV mass and wall thickness using machine learning algorithms serves both a practical and time-saving purpose. For instance, patients with contraindications for cardiac MRI, such as those with pacemakers, claustrophobia, or conditions prohibiting prolonged MRI examinations could potentially benefit from CCTA as prior mentioned factors play no role in CCTA acquisition (9). Furthermore, the increased availability, cost-effectiveness and speed of CCTA compared to cardiac MRI make it an attractive alternative for routine clinical use (12, 13). Lastly, LV segmentation is time consuming and machine learning algorithms for automatic LV segmentation have already been proved to speed up this process (14, 16, 17). An important consideration is whether use of these algorithms does not compromise the accuracy of LV segmentation as compared to the gold standard of cardiac MRI.

4. Results

CCTA -and cardiac MRI images from 57 participants were used in the current analysis hence a total of a 114 scans were analysed. Table 1 lists a detailed description of patient characteristics. Mean LV mass derived from CCTA and cardiac MRI including the standard deviation were 127 ± 31.6 and 128 ± 31.0 g, respectively. Mean wall thickness derived from CCTA and cardiac MRI including the standard deviation were 7 ± 1.5 mm and 8 ± 1.3 mm, respectively. Correlation between CCTA and cardiac MRI derived LV mass was very strong ($r = 0.908$, $p < 0.001$). Furthermore, corresponding mean differences and 95% limits of agreement for LV mass as demonstrated by the Bland-Altman plot were -1.26 (25.06;-27.58). LV wall thickness correlation between CCTA and cardiac MRI was strong ($r = 0.644$, $p < 0.001$) for average wall thickness and ($r = 0.662$, $p < 0.001$), ($r = 0.668$, $p < 0.001$) for the basal and mid regions, respectively. Average wall thickness in the apical regions demonstrated a moderate correlation ($r = 0.524$, $P < 0.001$). Corresponding mean differences and 95% limits of agreement were -0.57 (1.78;-2.92), -0.75 (1.34;-2.83), -0.58 (2.14;-3.30) and -0.29 (3.21;-3.79) for average wall thickness, basal, mid and apical regions, respectively. The average value for the thickest segments on MRI and CCTA including the standard deviation were 11 ± 1.8 and 10 ± 2.5 mm respectively and demonstrated a strong correlation ($r=0.687$ $p<0.001$). Corresponding mean differences and 95% limits of agreement were -1.06 (2.47;-4.60). Relevant charts for LV mass and wall thickness

correlations between CCTA and MRI as well as limits of agreement including mean difference are depicted in figure 4, figure 5, figure 6 and figure 7. All results are listed numerically in Table 2 as well as LV mass and LV wall thickness values according to clinical diagnosis in Table 3.

Mean differences per segment were assessed using the standard 16-segment model. Results are depicted in figure 8.

Interobserver correlations and intraclass correlation coefficients for CCTA derived LV mass, MRI derived LV mass, CCTA derived average wall thickness and MRI derived average wall thickness were excellent yielding Pearson's correlations coefficients of ($r = 0.994$, $p < 0.001$), ($r = 0.970$, $p < 0.001$), ($r = 0.971$, $p < 0.001$), ($r = 0.956$, $p < 0.001$), ($r = 0.965$, $p < 0.001$) ($r = 0.877$, $p < 0.001$), ($r = 0.825$, $p < 0.001$) and ($r = 0.820$, $p < 0.001$) respectively.

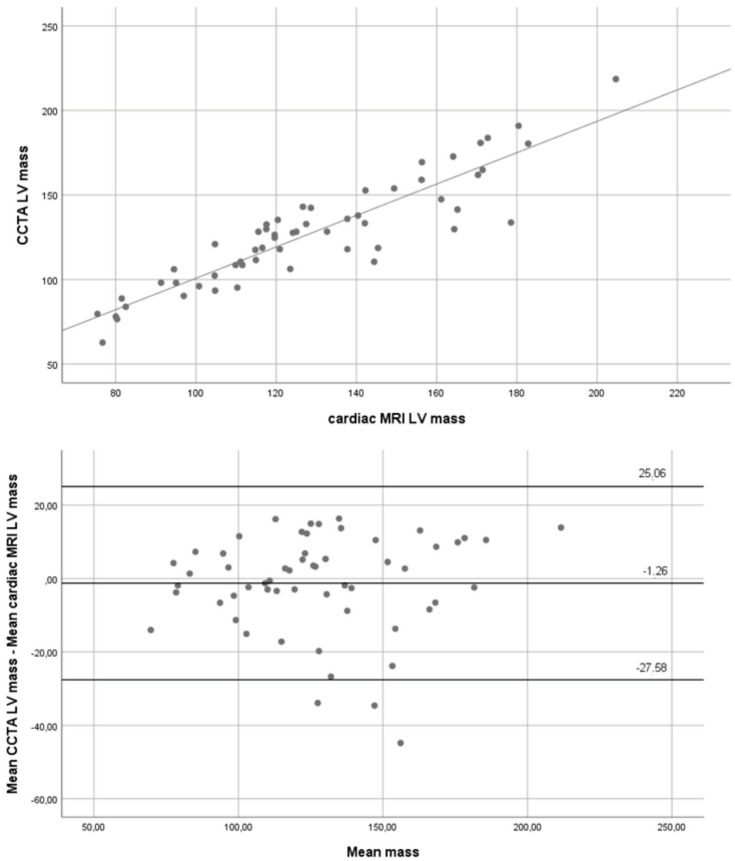

Figure 4. Correlations and mean differences with corresponding 95% limits of agreement for mean LV mass in grams. CCTA: Cardiac computed tomography angiography. MRI: Magnetic resonance imaging. LV: Left ventricle.

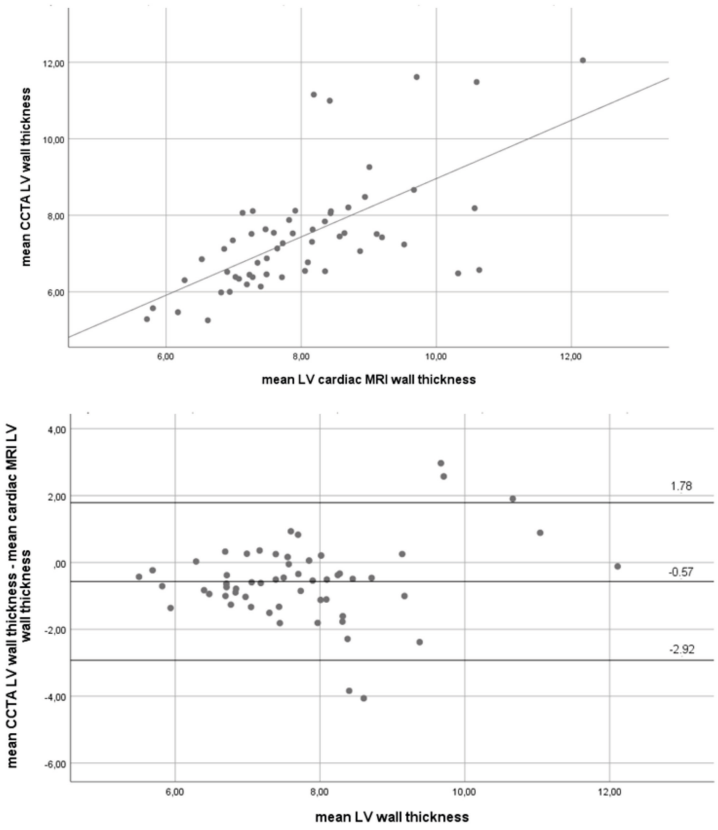

Figure 5. Correlations and mean differences with corresponding 95% limits of agreement for mean LV wall thickness in millimeters. CCTA: Cardiac computed tomography angiography. MRI: Magnetic resonance imaging. LV: Left ventricle.

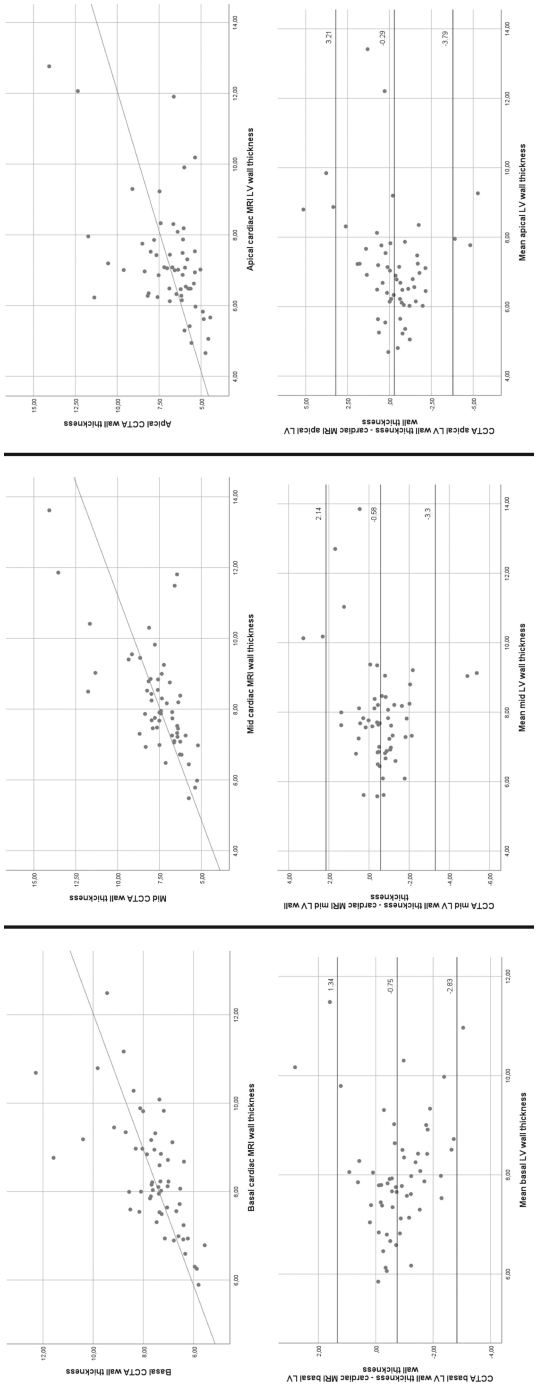

Figure 6. Correlations and mean differences with corresponding 95% limits of agreement for mean LV wall thickness in millimeters according to regions. CCTA: Cardiac computed tomography angiography. MRI: Magnetic resonance imaging. LV: Left ventricle.

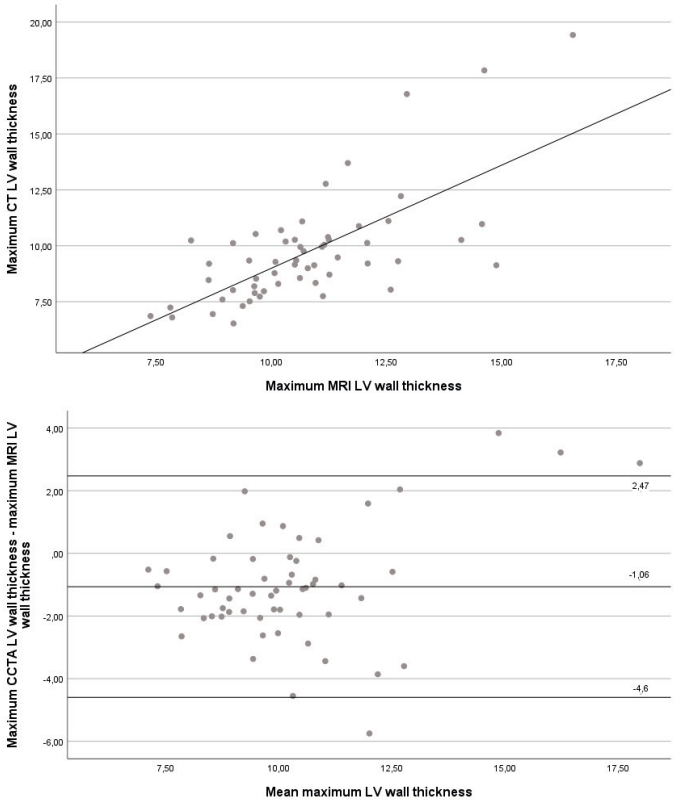

Figure 7. Correlations and mean differences with corresponding 95% limits of agreement for LV wall thickness differences corresponding to the thickest segments in millimeters. CCTA: Cardiac computed tomography angiography. MRI: Magnetic resonance imaging.

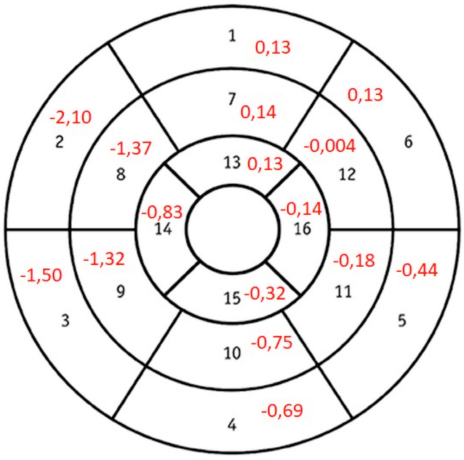

Figure 8. Mean differences in millimeters between CCTA and MRI wall thickness per segment are represented by the red numbers.

Table 2

	Pearson's correlation coefficient R	Mean differences and 95% limits of agreement
LV mass	0.908 (p<0.001)	-1.26 (25.06;-27.58)
LV wall thickness entire LV	0.644 (p<0.001)	-0.57 (1.78;-2.92)
LV wall thickness basal region	0.662 (p<0.001)	-0.75 (1.34;-2.83)
LV wall thickness mid region	0.668 (p<0.001)	-0.58 (2.14;-3.30)
LV wall thickness apical region	0.524 (p<0.001)	-0.29 (3.21;-3.79)
Maximum LV wall thickness	0.687 (p<0.001)	-1.06 (2.47;-4.60).

Correlations and limits of agreement between CCTA and MRI. LV: Left ventricle.

Table 3

Diagnosis	Average CCTA LV mass	Average MRI LV mass	Average CCTA LV wall thickness	Average MRI LV wall thickness
Diabetes mellitus (N=3)	130 grams	123 grams	9 mm	8 mm
Hypertension (N=24)	135 grams	137 grams	8 mm	9 mm
Hyperlipidaemia (N=12)	142 grams	140 grams	9 mm	9mm

Average LV mass and wall thickness on CCTA and MRI according to comorbidity. CCTA: Cardiac computed tomography angiography. LV: Left ventricle. MRI: Magnetic resonance imaging.

5. Discussion

This study assessed the comparison of LV mass and LV wall thickness between CCTA and cardiac MRI calculated from LV epi- and endocardial contours whilst using machine learning algorithms for automatic placement of these contours. Results demonstrate that CCTA shows good correlation with MRI with regard to LV mass and LV wall thickness. Also, Bland-Altman plots show narrow limits of agreement and minimal bias. As a result, (CCTA) can serve not only in the evaluation of coronary stenoses but also in the assessment of LV mass and wall thickness. This capability positions CCTA as a viable alternative to cardiac MRI.

Koo et al. performed an analysis in which they evaluated the accuracy of a deep learning-based algorithm for the segmentation of the LV on CCTA. However, instead of comparing this to MRI the results were compared to manual segmentations. It was demonstrated that deep learning-based segmentation results were comparable to those provided by manual segmentation with a high Dice index. They also concluded that based on visual analysis, automated LV segmentation using deep learning is superior to semi-automatic segmentation performed by an expert reader. Unfortunately, no statistical evidence was given to back up this last claim (14).

In a comprehensive review by Kawel et al. reference values of LV mass were given for cardiac MRI. An average LV mass of 121 grams was found for men and 83 grams for women. As the goal of our study was to assess the agreement of LV mass and LV wall thickness between CCTA and MRI men and women were not assessed separately. Still, our average LV mass value on cardiac MRI of 128 g closely matches the value found by Kawel et al. Given the predominant representation of men in our study (75 vs. 25% women), it is noteworthy that this gender distribution imbalance could contribute to an elevated average LV mass value, given the generally higher LV mass observed in men compared to women (22). It is also important to realize that due to the retrospective nature of this study the cohort consists of clinical participants, hence we cannot exclude the possibility of this cohort having a higher than average LV mass as compared to a sample of the general population which was used by Kawel et al. Furthermore, in another study by Kawel et al. the normal values for LV wall thickness on cardiac MRI were assessed per segment according to the standard 16-segment model. An average of 6 and 7 mm were found respectively for women and men when combining all regions. This closely matches our result of 8 mm for average LV wall thickness. Again, the result in our study could be slightly higher due to the fact that we have included vastly more men than women (19, 21) and that due to the retrospective nature of this study the cohort consists of clinical participants which may have a higher average LV mass as compared to the general population.

A study by Kara et al. also compared myocardial LV mass between CCTA and MRI using manual LV contour tracing for both modalities. It was also found that LV mass derived from CCTA correlated strongly with cardiac MRI using Pearson's correlation coefficient ($r = 0.884$, $p < 0.001$), which is comparable to our study. Furthermore, Bland-Altman plots by Kara et al. demonstrated a mean difference of 19.50 g with corresponding 95% upper and lower limits of agreement of 66.05 and -27.05 g, respectively (9). The difference between the upper limit and the lower limit in our study for LV mass as well as the mean difference is much lower as compared to Kara et al. This could be attributed to the fact that Kara et al. used a 64 slice computed tomography (CT) scanner whereas in our study this was a 320 slice CT scanner greatly increasing image quality (23). Also, no machine learning model was used for LV segmentation in the study by Kara et al.

Wang et al. similarly used automatic software for LV wall thickness comparison between CCTA and cardiac MRI. The methodology of our study is comparable to the study by Wang et al. as the borders of the endocardium and epicardium were automatically segmented. However, MRI contours were segmented manually. A Pearson's correlation coefficient for average LV wall thickness between CCTA and cardiac MRI of $r = 0.698$ ($p < 0.01$) was found by Wang et al. This is slightly higher compared to ours $r = 0.644$ ($p < 0.01$). However, Bland-Altman plots obtained by Wang et al. revealed a mean difference of 0.6 mm with 95% upper and lower limits of agreement of 4.0 mm and -2.7 mm, respectively (8). Although the mean difference is equivalent to our study, their observed difference between the upper and lower limits is considerably more than in our study. Again, this could be partly

explained due to the use of different scanner settings. Unfortunately, the slice capacity of the scanner used was not provided by Wang et al.

Given the Bland-Altman plots for mass differences between CCTA and MRI in our study it is important to note how these upper and lower limits would affect the diagnosis of LV hypertrophy. For instance, Levy et al. investigated the cut-off values for LV mass that define LV hypertrophy. It was found that a LV mass of 294 g or more for men and 198 g or more for women would implicate LV hypertrophy. Our study found mean LV mass of 127 and 128 g for CCTA and cardiac MRI respectively and 95% limits of agreement for differences between CCTA and cardiac MRI of 25.06;-27.58 implicate that diagnosing LV hypertrophy would still be possible as potential differences between CCTA and cardiac MRI measurements are well below that of LV hypertrophy (24).

Interestingly, when observing the mean differences between CCTA and cardiac MRI derived wall thickness per segment in Figure 8 it can be observed that the mean differences are greater in septal regions compared to other regions. This could be due to the fact that on cardiac MRI it is easier to differentiate between the septum wall and the RV as compared to CCTA as with the latter there is less contrast in the RV as compared to the LV (25). Furthermore, it is observed that correlation coefficient and limits of agreement considering wall thickness on CCTA and cardiac MRI are less strong for the apical region compared to other regions. This is mainly due to the fact that smaller contours which are more present apically are more prone to bias as was also described by Mitchell et al (26).

5.1 Limitations

This study has several limitations, which are innate to its retrospective design and novel nature. Firstly, it was conducted at a single centre, which may limit the generalizability of our findings to broader patient populations and clinical settings. Consequently the sample size in our study was limited, which may affect the statistical power and precision of our results. Secondly, the absence of clinical endpoints in our study restricts our ability to directly assess the impact of CCTA compared to cardiac MRI on patient outcomes. Thirdly, it was not possible to use similar cardiac gating parameters for the CCTA and cardiac MRI. Hence, differences in LV mass and LV wall thickness between CCTA and cardiac MRI may be attributed due to differences in the cardiac timing of the image acquisition. Still for both imaging modalities the phase on 75% of the RR interval was used for contour placement and subsequent LV mass and wall thickness comparison. However, differences in heartbeat may still have negatively impacted equal cardiac timing of CCTA and cardiac MRI. It is worth noting that different scanners with different tesla strengths (1.5 and 3.0 T) were used for MRI image acquisition in our study. Although using a 3.0 T scanner can substantially decrease scanning time compared to a 1.5 T scanner it has been demonstrated that there is no difference regarding LV mass and wall thickness measurements. Therefore use of different MRI scanners in this study is unlikely to have influenced the LV contour placement accuracy (27). Fourthly, images derived from CCTA

and MRI have a different slice thickness. We cannot entirely exclude the possibility that this has influenced the accuracy of LV contour placement. However, multiple studies have demonstrated that the accuracy of LV segmentation is not affected by slice thickness both for CCTA and MRI (28, 29). Lastly, In our study, we deliberately chose not to include papillary muscles and trabeculae in the LV mass assessment as our primary objective was to conduct a uniform comparison between cardiac MRI and CCTA for LV mass and wall thickness quantification. Furthermore, including papillary muscles and trabeculae in the assessment is time consuming and may introduce variability, potentially confounding the comparison between the two imaging modalities (30). Still, not including papillary muscles and trabeculae may have introduced bias as this can lead to lower LV volumes as compared to the reference values, especially in patients with LV hypertrophy (30).

6. Conclusions

Utilizing CCTA for assessment of LV mass and wall thickness whilst using a machine learning model for LV segmentation shows good agreement with cardiac MRI. Consequently, CCTA may offer a reliable alternative for individuals with contraindications to cardiac MRI in the context of LV mass and wall thickness assessment. Notably, CCTA offers advantages in terms of greater accessibility, cost-effectiveness, and faster imaging acquisition compared to MRI (12, 13), albeit with the caveat of increased radiation exposure (31). Despite being conducted at a single center and without clinical endpoints, our findings offer important preliminary evidence that warrants further investigation and validation in larger, multicenter studies with clinical outcomes.

References

1. Haider AW, Larson MG, Benjamin EJ, Levy D. Increased left ventricular mass and hypertrophy are associated with increased risk for sudden death. J Am Coll Cardiol. 1998;32(5):1454-9.
2. Fulton N, Rajiah P. Utility of magnetic resonance imaging in the evaluation of left ventricular thickening. Insights Imaging. 2017;8(2):279-93.
3. Opincariu D, Benedek T, Chitu M, Rat N, Benedek I. From CT to artificial intelligence for complex assessment of plaque-associated risk. Int J Cardiovasc Imaging. 2020;36(12):2403-27.
4. Budoff MJ, Ahmadi N, Sarraf G, Gao Y, Chow D, Flores F, et al. Determination of left ventricular mass on cardiac computed tomographic angiography. Acad Radiol. 2009;16(6):726-32.
5. Klein R, Ametepe ES, Yam Y, Dwivedi G, Chow BJ. Cardiac CT assessment of left ventricular mass in mid-diastasis and its prognostic value. Eur Heart J Cardiovasc Imaging. 2017;18(1):95-102.
6. Khatri PJ, Tandon V, Chen L, Yam Y, Chow BJ. Can left ventricular end-diastolic volumes be estimated with prospective ECG-gated CT coronary angiography? Eur J Radiol. 2012;81(2):226-9.
7. Juneau D, Erthal F, Clarkin O, Alzahrani A, Alenazy A, Hossain A, et al. Mid-diastolic left ventricular volume and mass: Normal values for coronary computed tomography angiography. J Cardiovasc Comput Tomogr. 2017;11(2):135-40.
8. Wang R, Meinel FG, Schoepf UJ, Canstein C, Spearman JV, De Cecco CN. Performance of Automated Software in the Assessment of Segmental Left Ventricular Function in Cardiac CT: Comparison with Cardiac Magnetic Resonance. Eur Radiol. 2015;25(12):3560-6.
9. Kara B, Nayman A, Guler I, Gul EE, Koplay M, Paksoy Y. Quantitative Assessment of Left Ventricular Function and Myocardial Mass: A Comparison of Coronary CT Angiography with Cardiac MRI and Echocardiography. Pol J Radiol. 2016;81:95-102.
10. Andreini D, Conte E, Mushtaq S, Melotti E, Gigante C, Mancini ME, et al. Comprehensive Evaluation of Left Ventricle Dysfunction by a New Computed Tomography Scanner: The E-PLURIBUS Study. JACC Cardiovasc Imaging. 2023;16(2):175-88.
11. Alnasser TN, Abdulaal L, Maiter A, Sharkey M, Dwivedi K, Salehi M, et al. Advancements in cardiac structures segmentation: a comprehensive systematic review of deep learning in CT imaging. Front Cardiovasc Med. 2024;11:1323461.
12. Papanicolas I, Woskie LR, Jha AK. Health Care Spending in the United States and Other High-Income Countries. JAMA. 2018;319(10):1024-39.
13. Tidwell AS, Jones JC. Advanced imaging concepts: a pictorial glossary of CT and MRI technology. Clin Tech Small Anim Pract. 1999;14(2):65-111.
14. Koo HJ, Lee JG, Ko JY, Lee G, Kang JW, Kim YH, et al. Automated Segmentation of Left Ventricular Myocardium on Cardiac Computed Tomography Using Deep Learning. Korean J Radiol. 2020;21(6):660-9.
15. Lu YL, Connelly KA, Dick AJ, Wright GA, Radau PE. Automatic functional analysis of left ventricle in cardiac cine MRI. Quant Imaging Med Surg. 2013;3(4):200-9.
16. van Driest FY, Bijns CM, van der Geest RJ, Broersen A, Dijkstra J, Jukema JW, et al. Correlation between quantification of myocardial area at risk and ischemic burden at cardiac computed tomography. Eur J Radiol Open. 2022;9:100417.
17. Alabed S, Alandejani F, Dwivedi K, Karunasaagarar K, Sharkey M, Garg P, et al. Validation of Artificial Intelligence Cardiac MRI Measurements: Relationship to Heart Catheterization and Mortality Prediction. Radiology. 2022;304(3):E56.
18. Abbara S, Blanke P, Maroules CD, Cheezum M, Choi AD, Han BK, et al. SCCT guidelines for the performance and acquisition of coronary computed tomographic angiography: A report of the society of Cardiovascular Computed Tomography Guidelines Committee: Endorsed by the North American Society for Cardiovascular Imaging (NASCI). J Cardiovasc Comput Tomogr. 2016;10(6):435-49.
19. Kawel N, Turkbey EB, Carr JJ, Eng J, Gomes AS, Hundley WG, et al. Normal left ventricular myocardial thickness for middle-aged and older subjects with steady-state free precession cardiac magnetic resonance: the multi-ethnic study of atherosclerosis. Circ Cardiovasc Imaging. 2012;5(4):500-8.
20. Isma'eel H, Hamirani YS, Mehrinfar R, Mao S, Ahmadi N, Larijani V, et al. Optimal phase for coronary interpretations and correlation of ejection fraction using late-diastole and end-diastole imaging in cardiac computed tomography angiography: implications for prospective triggering. Int J Cardiovasc Imaging. 2009;25(7):739-49.

21. Cerqueira MD, Weissman NJ, Dilsizian V, Jacobs AK, Kaul S, Laskey WK, et al. Standardized myocardial segmentation and nomenclature for tomographic imaging of the heart. A statement for healthcare professionals from the Cardiac Imaging Committee of the Council on Clinical Cardiology of the American Heart Association. Circulation. 2002;105(4):539-42.
22. Kawel-Boehm N, Hetzel SJ, Ambale-Venkatesh B, Captur G, Francois CJ, Jerosch-Herold M, et al. Reference ranges ("normal values") for cardiovascular magnetic resonance (CMR) in adults and children: 2020 update. J Cardiovasc Magn Reson. 2020;22(1):87.
23. Khan A, Khosa F, Nasir K, Yassin A, Clouse ME. Comparison of radiation dose and image quality: 320-MDCT versus 64-MDCT coronary angiography. AJR Am J Roentgenol. 2011;197(1):163-8.
24. Levy D, Savage DD, Garrison RJ, Anderson KM, Kannel WB, Castelli WP. Echocardiographic criteria for left ventricular hypertrophy: the Framingham Heart Study. Am J Cardiol. 1987;59(9):956-60.
25. Lee H, Kim SY, Gebregziabher M, Hanna EL, Schoepf UJ. Impact of ventricular contrast medium attenuation on the accuracy of left and right ventricular function analysis at cardiac multi detector-row CT compared with cardiac MRI. Acad Radiol. 2012;19(4):395-405.
26. Mitchell SC, Bosch JG, Lelieveldt BP, van der Geest RJ, Reiber JH, Sonka M. 3-D active appearance models: segmentation of cardiac MR and ultrasound images. IEEE Trans Med Imaging. 2002;21(9):1167-78.
27. Gandy SJ, Lambert M, Belch J, Cavin I, Crowe E, Littleford R, et al. 3T MRI investigation of cardiac left ventricular structure and function in a UK population: The tayside screening for the prevention of cardiac events (TASCFORCE) study. Journal of Magnetic Resonance Imaging. 2016;44(5):1186-96.
28. DOĞAN H, VELDKAMP WJH, DIBBETS-SCHNEIDER P, SPIJKERBOER AM, MERTENS BJA, KROFT LJM, et al. Effects of heart rate, filling and slice thickness on the accuracy of left ventricular volume measurements in a dynamic cardiac phantom using ECG-gated MDCT. The British Journal of Radiology. 2008;81(967):577-82.
29. Higgins CB, de Roos A. MRI and CT of the Cardiovascular System: Lippincott Williams & Wilkins; 2006.
30. Yang C, Xu H, Qiao S, Jia R, Jin Z, Yuan J. Papillary and Trabecular Muscles Have Substantial Impact on Quantification of Left Ventricle in Patients with Hypertrophic Obstructive Cardiomyopathy. Diagnostics (Basel). 2022;12(8).
31. Hausleiter J, Meyer T, Hermann F, Hadamitzky M, Krebs M, Gerber TC, et al. Estimated Radiation Dose Associated With Cardiac CT Angiography. JAMA. 2009;301(5):500-7.
32. Ommen SR, Mital S, Burke MA, Day SM, Deswal A, Elliott P, et al. 2020 AHA/ACC Guideline for the Diagnosis and Treatment of Patients With Hypertrophic Cardiomyopathy: Executive Summary: A Report of the American College of Cardiology/American Heart Association Joint Committee on Clinical Practice Guidelines. Circulation. 2020;142(25):e533-e57.